Journal of Inorganic and General Chemistry
ZAAC
Zeitschrift für anorganische und allgemeine Chemie

DOI: 10.1002/zaac.202000123

ARTICLE

Combining Performance with Thermal Stability: Synthesis and Characterization of 5-(3,5-Dinitro-1*H*-pyrazol-4-yl)-1*H*-tetrazole and its Energetic Derivatives

Maximilian Benz,[a] Thomas M. Klapötke,*[a] and Jörg Stierstorfer[a]

Dedicated to Professor Christian Robl on the Occasion of his 65th Birthday

Abstract. In this study, we present the synthesis of 5-(3,5-dinitro-1*H*-pyrazol-4-yl)-1*H*-tetrazole and its energetic derivatives starting from 4-amino-3,5-dinitropyrazole, which was diazotized and cyanide substituted. A subsequent cycloaddition reaction with sodium azide led to 5-(3,5-dinitro-1*H*-pyrazol-4-yl)-1*H*-tetrazole (**3**). Several alkaline metal and nitrogen-rich salts were prepared and characterized by low-temperature X-ray diffraction. Additionally, all compounds were analyzed by vibrational spectroscopy (IR), ^{1}H, ^{13}C and ^{14}N NMR spectroscopy, elemental analysis and differential thermal analysis (DTA). Additionally, the heats of formation for selected compounds were calculated using the atomization method based on CBS-4M enthalpies as well as important detonation parameters by using the EXPLO5 code (V6.05). Furthermore, the sensitivities of **3** and all synthesized salts toward friction, impact and electrostatic discharge according to BAM (*Bundesamt für Materialforschung*) were determined and compared to RDX.

Introduction

The demand for new energetic materials has risen sharply in recent years, as the field of application has been extended not only to the military sector, but also to an increasing number of civilian sectors, such as aerospace technology and the automotive industry.[1–3] Increasingly specialized fields of application also constantly present new challenges in the development of suitable substances.[4,5] Some key characteristics every new HEDM to be developed should meet are a high decomposition temperature, which is especially important for temperature resistant materials. In addition, paired with low sensitivity to external stimuli, this is indispensable for the safety of the persons handling the materials.[6–8] Green chemistry is also becoming an increasingly important point to consider in the development of energetic materials.[3,9,10] Newly developed materials should therefore be completely free of toxic or environmentally harmful reactants in their synthesis. Of course, the toxicity of the final product is also important and should therefore be as harmless as possible.[11–13] Especially for the military sector, more performance-efficient substances are of interest.[5] In addition, production costs must be regarded as a criterion, as the tendency here is to produce larger quantities. The latter is particularly easy to achieve if the starting materials are easily available and rapidly accessible.[14,15]

Especially azoles like pyrazoles, triazoles, tetrazoles or oxygen containing five-membered heterocycles like furazan or oxadiazoles have proven to be good building blocks of novel energetic materials.[17–21] Pyrazoles are particularly suitable because they have a relatively high heat of formation (HoF) and still exhibit high thermal stability, which is due to the three linked carbon atoms. In addition, energetic modifications, such as nitration or oxidation, can be carried out rather simply[22,23] (Figure 1a).

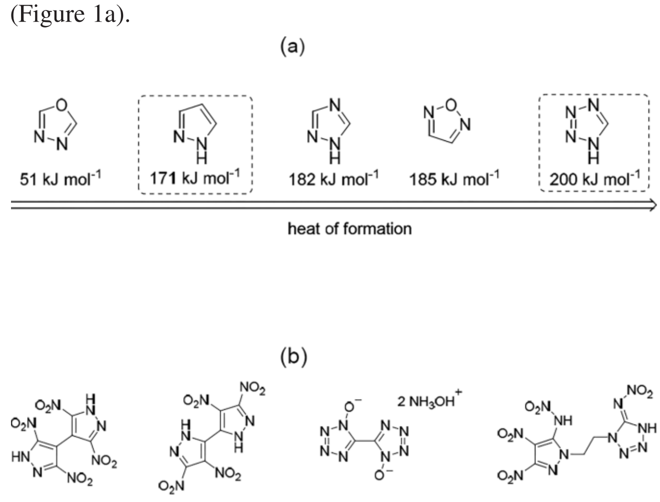

Figure 1. (a) Gas-phase heats of formation for selected azoles and oxadiazoles.[9,16] (b) Literature known explosives based on linked pyrazoles and tetrazoles: TN-4,4'-BP (tetranitro-4,4'-bipyrazole),[26] TN-3,3'-BP (tetranitro-3,3'-bipyrazole),[27] TKX-50 (dihydroxylammonium 5,5′-bitetrazole-1,1′-dioxide),[14] DNNPENT (*N*-(1-(2-(3,4-dinitro-5-(nitroamino)-pyrazol-1-yl)ethyl)-5*H*-tetrazol-5-ylidene)-nitramide).[28]

* Prof. Dr. T. M. Klapötke
E-Mail: tmk@cup.uni-muenchen.de
www.hedm.cup.uni-muenchen.de
[a] Department of Chemistry
Univeristy of Munich (LMU)
Butendandtstr. 5–13 (D)
81377 München, Germany

Supporting information for this article is available on the WWW under **http://dx.doi.org/10.1002/zaac.202000123** or from the author.

Tetrazole building blocks are attractive due to their extremely high nitrogen content and by a large heat of formation.[24,25] Although there are many examples of bridged pyrazoles, tetrazoles or combinations thereof (Figure 1b), no C–C linked and fully functionalized pyrazole-tetrazole hybrid, which at best combines the positive properties of the individual building blocks, is yet known.

Energetic materials based on the 5-(pyrazol-4-yl)-tetrazole skeleton have not been mentioned in literature yet. Herein, we report on the synthesis of the first compound combining a dinitropyrazole derivative with a tetrazole via a C–C bond in a five-step reaction. In addition, various mono salts of H_2DNPT (**3**) were synthesized and intensively characterized and compared to each other.

Results and Discussion

Synthesis

The synthesis of 5-(3,5-dinitro-1*H*-pyrazol-4-yl)-1*H*-tetrazole (H_2DNPT, **3**) starts with the chlorination of 1*H*-pyrazole using in situ generated chlorine (NaOCl/HCl; Scheme 1) to form 4-chloro-pyrazole.[22,29] A subsequent nitration using a mixture of sulfuric acid and fuming nitric acid formed 4-chloro-3,5-dinitropyrazole.[22,30,31] The third step was performed in an steel autoclave using aqueous ammonia to yield 4-amino-3,5-dinitropyrazole (ADNP, **1**).[22,30,31] ADNP was diazotated in diluted sulfuric acid using sodium nitrite. After neutralization with sodium carbonate the in situ generated diazonium group was substituted by cyanide by an reductive elimination reaction to form 4-cyano-3,5-dinitropyrazole (**2**) as sodium salt. H_2DNPT (**3**) was obtained by a reaction using a modified procedure of *Sharpless* and co-workers, which has a broad approach in the synthesis of C–C fused tetrazole azole compounds.[18,32–34] The [3+2] cycloaddition of NaCDNP (**2**) with sodium azide and zinc chloride as catalyst in water yields **3** in 55 % yield. The corresponding energetic salts of H_2DNPT were produced by diluting the neutral compound in water, alcohol (MeOH, EtOH) or mixtures of those and subsequent addition of one equivalent of the corresponding base (Scheme 1C). The respective salts precipitated immediately or were obtained by evaporation of the solvent in very good yields and high purities.

All compounds were fully characterized by IR and multinuclear NMR spectroscopy, mass spectrometry and differential thermal analysis. Further, selected compounds were analyzed using low-temperature single-crystal X-ray measurements.

Crystal Structures

Suitable crystals of compounds **2–5**, **7**, **8**, **11** and **12** were obtained by recrystallization of the crude products from methanol or acetonitrile, respectively. Compounds **2**, **11** and **12** crystallize with the inclusion of water molecules. The DAU and hydrazinium derivatives **9** and **10** maintained crystalline morphology, but the solution of the diffraction measurement data could not be completed due to structural disorder. Here, only the low temperature X-ray crystal structures of the neutral compound **3** and anhydrous derivatives **4**, **5**, **7** and **8** are discussed. The other solid-state structures can be found in the Supporting Information.

Compound **3** crystallizes in the orthorhombic space group *Pbca* with a cell volume of 1754.19(12) Å^3 and eight formula units per cell. The cell constants are a = 9.5893(3) Å, b = 10.5373(5) Å and c = 17.3604(7) Å, while the density is 1.712 g cm^{-3} at 123 K. Thus, the density is clearly below the value calculated by *Ghule* et al.[35] The nitro groups are almost in one plane with the pyrazole moiety (O2–N3–C3–C2 –3.9°, O3–N4–C1–N2 –2.4°). The pyrazole and tetrazole ring of H_2DNPT each have a planar structure (C3–N1–N2–C1 0.6°, N6–N5–C4–N8 0.2°). However, both rings in the molecule are not coplanar to each other (C1–C2–C4–N8 129°). The twisting

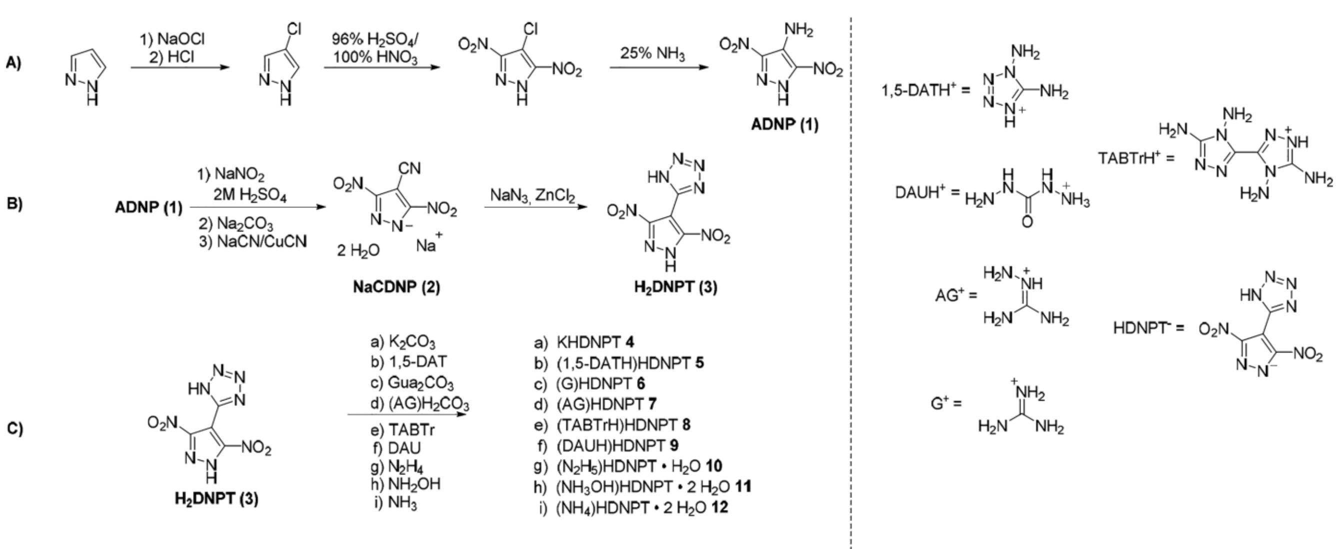

Scheme 1. (A) Literature know synthesis of 4-amino-3,5-dinitropyrazole (ADNP, **1**). (B) Synthesis of 5-(3,5-dinitro-1*H*-pyrazol-4-yl)-1*H*-tetrazole (**3**). (C) Synthesis of new energetic salts of H_2DNPT.

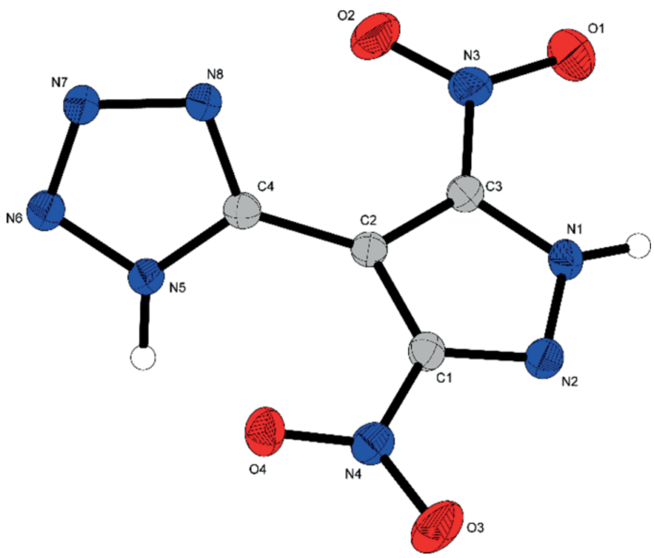

Figure 2. Molecular unit of compound **3**, showing the atom labeling scheme. Thermal ellipsoids represent the 50 % probability level and hydrogen atoms are shown as small spheres of arbitrary radius. Selected bond lengths /Å and angles /°: C2–C4 1.465(2), C1–N4 1.4445(19), C3–N3 1.444(2), O3–N4–C1 116.80(12), O2–N3–C3 117.61(12), O2–N3–C3–C2 –3.9(2), O3–N4–C1–N2 –2.4(2), C1–C2–C4–N8 129.02(17).

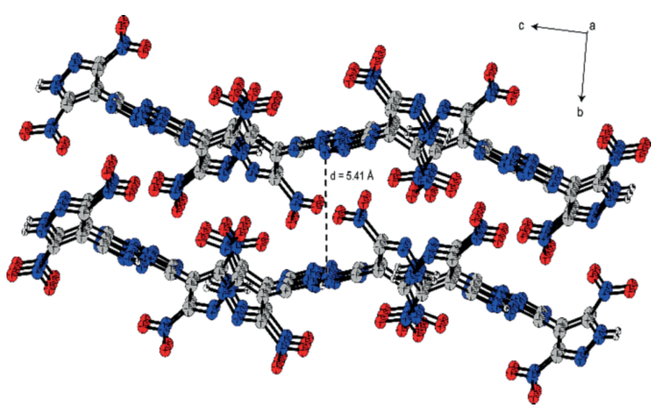

Figure 3. Stacking of layers of compound **3** (layer distance d = 5.41 Å). Thermal ellipsoids are drawn at the 50 % probability level.

prevents a regular stacking of the molecular units. This can be assumed to be the main reason for the low density of compound **3** (1.669 g cm^{-3} at 298 K). The bond lengths within the azole rings are between the expected values for C–C, C–N and N–N single and double bonds (C–C:1.47 Å, 1.34 Å, C–N: 1.47 Å, 1.22 Å; N–N: 1.48 Å, 1.20 Å).[36–37] The C–C bond between the two aromatic rings has the classic length of a single bond (C2–C4 1.465 Å)[36,38] (Figure 2, Figure 3, and Figure 4).

Compound **3** forms a wave-like layering structure along c, with a layer distance of 5.41 Å. The only classical hydrogen bridges are between the acidic protons and the nitrogen atoms of the tetrazole moiety. The nitro groups do not form any intramolecular interactions in the structure. The tetrazole units form hydrogen bridges in direction of *a* axis N5–H5···N7^{iv} with a length of 1.96 Å and an angle of 166.2°. The molecular moieties in the *ac* plane form a strong intramolecular interaction with N8 at the tetrazole of the adjacent unit through the hydrogen at the pyrazole (N1–H1···N8^{iii}, 1.90 Å). The steric demand of the nitro groups also explains the tilting of the aromatic rings towards each other in the layering.

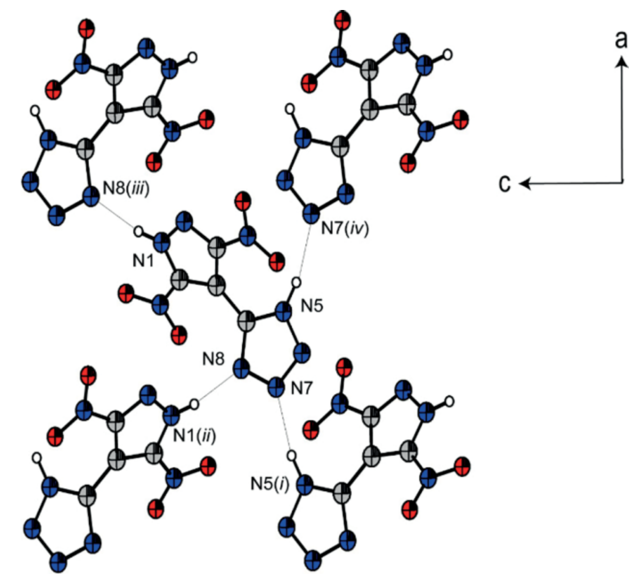

Figure 4. Formation of intramolecular hydrogen bonds of compound **3** along the *ac* plane; Symmetry codes: i) –0.5+x, 0.5–y, –z; ii) –0.5+x, y, 0.5–z; iii) 0.5+x, y, 0.5–z; iv) 0.5+x, 0.5–y, –z; Thermal ellipsoids are drawn at the 50 % probability level.

Compound **4** crystallizes is the monoclinic space group $P2_1$ with a cell volume of 910.47(8) Å^3 and two formula units per cell. The cell constants are a = 9.0333(4) Å, b = 11.3970(6) Å and c = 9.2529(4) Å, while the density is 1.928 g cm^{-3} at 131 K. Deprotonation occurs at the pyrazole ring, which indicates a more acidic character than the tetrazole proton. The pyrazole ring forms an almost flat plane with the two nitro groups (O3–N4–C3–N2 9.2°, O1–N3–C1–C2 176.6°). The ring moieties are not coplanar but around 61° tilted straight to each other. Compared to neutral compound **3**, the twist is more distinctive with about 10 degrees more. All bond lengths in the azole rings are in the range of C–C, C–N or N–N single and double bonds.[36] Compared to the neutral compound **3** the bond lengths do not vary significantly (Figure 5).

1,5-Diamino-tetrazol-4-ium 3,5-dinitro-4-(tetrazol-5-yl)pyrazolate (1,5-DATH)HDNPT (**5**) crystallizes in the monoclinic space group *C*2/*c* with a cell volume of 2395.10(25) Å^3 and eight molecular moieties in the cell unit. The molecular structure of **5** is presented in Figure 6.

The anions HDNPT$^-$ in **5** form dimers, which build two strong hydrogen bridges via the nitro group and the tetrazolium proton (N5^i–H5···O2, N5–H5···O1^i). Four further nitrogen atoms (i.e., N1, N2, N6 and N8) of the anion are involved as acceptor atoms in further hydrogen bonds (Table 1), thereby resulting strong interactions with surrounding cations. The donors of the hydrogen bridges originate from the amine functionalities N13 and N14 as well as the secondary tetrazole-amine N12.

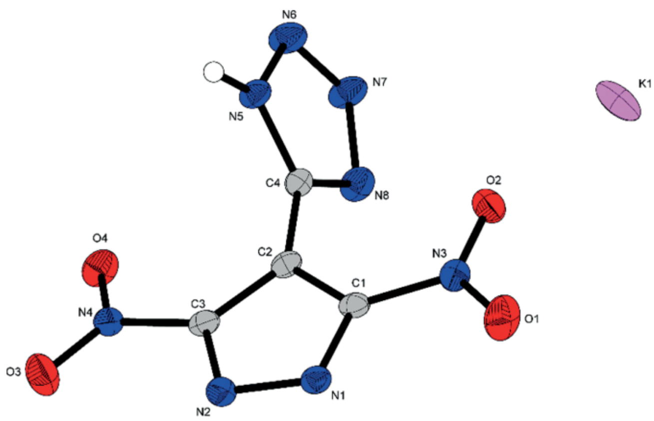

Figure 5. Molecular unit of compound **4**, showing the atom labeling scheme. Thermal ellipsoids represent the 50 % probability level and hydrogen atoms are shown as small spheres of arbitrary radius. Selected bond lengths /Å and angles /°: K1–O2 2.799(3), C2–C4 1.463(6), C3–N4 1.441(6), C1–N3 1.433(5), O2–N3–C1 117.7(3), O3–N4–C3 118.7(3), O3–N4–C3–N2 9.2(6), O1–N3–C1–C2 176.6(4), C3–C2–C4–N8 0.6(6).

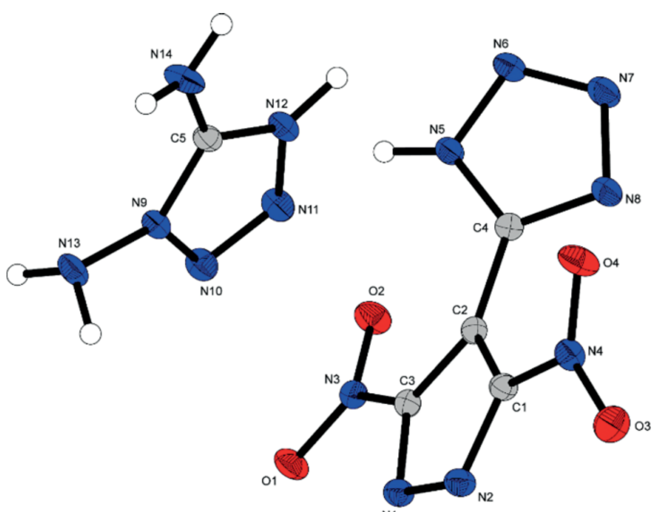

Figure 6. Molecular unit of compound **5**, showing the atom labeling scheme. Thermal ellipsoids represent the 50 % probability level and hydrogen atoms are shown as small spheres of arbitrary radius.

Furthermore, aminoguanidinium 3,5-dinitro-4-(tetrazol-5-yl) pyrazolate (AG)HDNPT (**7**) crystallizes water free in the orthorhombic space group *Pbcn* with eight molecular units per cell and a cell volume of 2263.21(13) Å^3. The molecular structure is shown in Figure 7. The crystal structure shows the formation of layers of cations and anions, respectively, along *c* axis. The anions $HDNPT^-$ create an alternating chain-like structure, whereby one clear interaction N5–H5···N1^i is built. Two aminoguanidinium cations surround the tetrazole ring and interact with the accepting nitrogen atoms N6 and N8. Another cation forms a strong interaction with the deprotonated pyrazole nitrogen (N1 and N2). Surprisingly, only one nitro group with O3 and O4 forms hydrogen bridges with the cation.

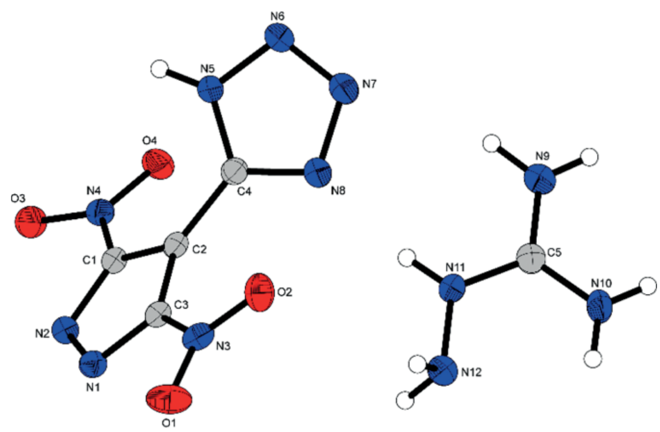

Figure 7. Molecular unit of compound **7**, showing the atom labeling scheme. Thermal ellipsoids represent the 50 % probability level and hydrogen atoms are shown as small spheres of arbitrary radius.

4,4′,5,5′-Tetraamino-[3,3′-bi(1,2,4-triazol)]-1-ium 3,5-dinitro-4-(tetrazol-5-yl)pyrazolate (TABTrH)HDNPT (**8**) crystallizes in the orthorhombic space group *Pna*2$_1$ with a cell volume of 1575.83(16) Å^3 and four molecular units per cell. The structure is depicted in Figure 8.

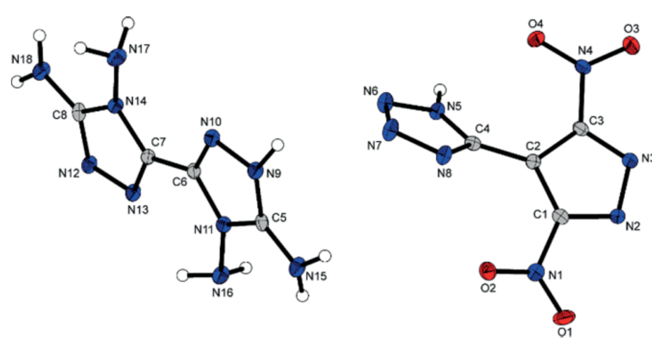

Figure 8. Molecular unit of compound **8**, showing the atom labeling scheme. Thermal ellipsoids represent the 50 % probability level and hydrogen atoms are shown as small spheres of arbitrary radius.

Table 1. Hydrogen bonds present in the crystal structure of **5**.

D–H···A	D–H /Å	H···A /Å	D–H···A /Å	D–H···A /°
N5^i–H5···O2	0.86(2)	2.58(2)	2.8736(18)	101.4(17)
N5–H5···O15^i	0.86(2)	2.14(2)	2.9561(17)	158(2)
N12^{ii}–H12···N2	0.92(2)	1.81(2)	2.7268(18)	174(2)
N13^{iii}–H13A···O4	0.89(2)	2.50(2)	3.1017(18)	126(2)
N13^{iv}–H13B···O2	0.89(2)	2.50(2)	3.1964(17)	132(2)
N13^v–H13B···N8	0.89(2)	2.39(2)	3.0859(19)	135(2)
N14^{iv}–H14A···N6	0.83(2)	2.27(2)	2.997(2)	146(2)
N14^{iv}–H14B···N1	0.86(2)	2.17(2)	3.0291(19)	175.2(18)

Symmetry codes: i) 1–x, 1–y, 1–z; ii) 3/2–x, 1/2 + *y*, 3/2–z; iii) x, 1–y, 1/2 + *z*; iv) –1/2 + *x*, 1/2 + *y*, z; v) 3/2–x, –1/2 + *y*, 3/2–z.

Both, the cations and the anions form linear chains along *c*. In the anion structure strong interactions between the tetrazoles are visible (N5–H5···N8^{i}). In the TABTrH chains, many interactions between the amines and the nitrogen atoms of the triazoles are detectable. In addition, certain hydrogen bridges between the accepting anion nitrogens N2, N3, N6 and N7 and the amino groups of the cation (N15–H15A, N15–H15B, N17–N17A, N18–H18A, N18–H18B) are formed.

NMR and Vibrational Spectroscopy

All compounds (**3–12**) were analyzed by ^{1}H, ^{13}C and ^{14}N spectroscopy with [D$_6$]DMSO as solvent (Table 2). Additionally, compound **3** was characterized by ^{15}N spectroscopy measurement.

The highly acidic protons of the pyrazole and tetrazole can only be detected as a broad signal at δ = 14.24 ppm for the neutral compound **3**. The signal only became detectable with an extended measuring time and high substance concentration, since a constant exchange takes place due to the high acidity in DMSO. For all deprotonated compounds (**4–12**), the remaining tetrazole proton signal could not be observed in the ^{1}H spectra. While the 1,5-DATH cation proton resonances in **5** are located at δ = 7.58 ppm resulting in a broad signal, the guanidinium compound **6**, representing 6 protons appears as sharp singlet at δ = 6.92 ppm. The aminoguanidinium cation shows four signals, in accordance to the four different types of protons, located at δ = 8.55 (N*H*–NH$_2$), 7.24 (NH$_2$), 6.72 (NH$_2$) and 4.68 ppm (NH–N*H*$_2$). The two different amino groups of the TABTrH cation can be assigned to sharp singlet signals at δ = 7.40 (N–N*H*$_2$) and 5.99 ppm (C–N*H*$_2$). The protons in the DAU compound **9** result in a broad signal at δ = 8.68 ppm. For the water containing compounds, the water signal can only be observed for the hydrazinium **10** and the hydroxylammonium **11** compound at δ = 3.36 and 3.39 ppm, respectively. Additionally, the cations of the water containing compounds show signals at δ = 7.13 ppm for the hydrazinium **10**, δ = 11.33 and 10.06 ppm for the hydroxylammonium **11** and δ = 7.24 ppm for the ammonium **12** compound.

In all ^{13}C NMR spectra one signal for the tetrazole and according to symmetry two signals for the pyrazole can be observed. The signals are all in the range for C-substituted tetrazoles and 3,5-dinitropyrazoles.[26,28,39,40] For the neutral compound **3** C4 can be observed at δ = 153.6 ppm, C1/C3 at δ = 147.3 ppm and C2 at δ = 97.5 ppm. The deprotonation of the pyrazole ring affects a shift of all carbon atoms. For C4 a down field shift can be monitored. The signals for all ionic compounds for C4 are between δ = 153.9 and 155.2 ppm. For C1/C3 the resonances are in the range of δ = 147.0 and 148.6 ppm. Except for the ammonium compound **12** (δ = 98.1 ppm) a trend to high field shift for C2 atoms is identifiable. The signals can be found at δ = 96.1 to 97.1 ppm. The signal for the carbon atom in the cation can be found at δ = 153.1 for **5** which is a usual shift for tetrazolium cations.[41] The guanidinium and aminoguanidinium derivatives show a resonance at δ = 157.9 and 158.8 ppm, respectively. The TABTr derivative has two more signals in the ^{13}C spectrum located at δ = 154.7 and 147.5 ppm. For the DAU salt the urea like carbon resonates at δ = 159.2 ppm.

The ^{14}N spectra of all compounds investigated compounds show the resonance for the nitro groups at the pyrazole. H$_2$DNPT (**3**) can be observed at δ = –24 ppm. The signals for the ionic species varies within the range of δ = –22 to –17 ppm. Compounds **11** and **12** show an additional signal at –359 ppm for the cation.

Figure 9 shows the ^{15}N NMR spectrum of compound **3**. The assignments were based on comparison with theoretical calculations using Gaussian 09[42] and literature values with similar 3,5-dinitropyrazoles and electron poor 5-substituted tetrazoles.[18,40,43] The spectrum shows two sharp signals at δ = –9.5 and –25.4 ppm. Additionally, two broad signals at δ = –93.8 and –98.0 ppm are observed. The sharp signals can be clearly assigned to the nitrogen N4/N4' (–9.5 ppm) of the tetrazole

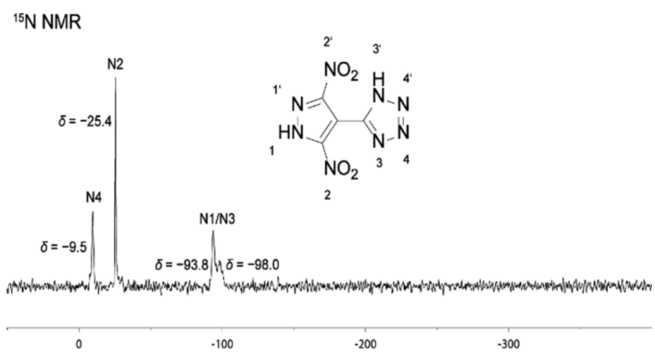

Figure 9. ^{15}N NMR spectra of H$_2$DNPT (**3**); chemical shifts are given in ppm.

Table 2. NMR resonances for compounds **3–12** measured in [D$_6$]DMSO.

Compound	δ /ppm ^{13}C	^{14}N	^{1}H
3	153.6, 147.3, 97.5	–24	14.24
4	154.7, 147.6, 96.4	–19	
5	153.9, 153.1, 147.0, 97.1	–22	7.58
6	157.9, 154.7, 147.6, 96.4	–20	6.92
7	158.8, 154.7, 147.5, 96.2	–20	8.55, 7.24, 6.72, 4.68
8	154.7, 153.9, 147.5, 138.6, 96.1	–20	7.40, 5.99
9	159.2, 154.7, 147.4, 96.1	–17	8.68
10·H$_2$O	154.8, 147.5, 96.2	–19	7.13, 3.36
11·2 H$_2$O	154.8, 147.5, 96.2	–19, –359	11.33, 10.06, 3.39
12·2 H$_2$O	155.2, 148.6, 98.1	–18, –359	7.24

moiety and the nitrogen atoms of the nitro groups N2/N2′ (–25.4 ppm). A defined assignment of the two wide signals to N1/N1′ and N3/N3′ is not possible. Due to the high acidity of the protons, no N–H couplings can be found in the spectrum. The associated rapid proton exchange in DMSO also explains the width of the signals.

The assignment of the respective oscillations in the IR spectra to the corresponding functional groups was checked with appropriate data.[44] The characteristic bands for the nitro groups (asymmetric and symmetric vibrations) can be found for all compounds investigated. They appear in the range of 1557–1514 cm^{-1} for the asymmetric stretching vibration and 1323–1312 cm^{-1} for the symmetric vibration, respectively. All compounds with an amino group containing cation (**5**–**9**) show significant absorption bands in the range of 3000 cm^{-1} for the NH_2 stretching vibration and in the region of 1600 cm^{-1} for the deformation vibration of the amino group.

Physicochemical Properties

As all compounds produced can be classified as energetic substances, the energetic properties must be investigated. The theoretically calculated and experimentally determined physicochemical values are shown in Table 3 and compared with the data of RDX. Computed values (detonation velocity, detonation pressure, ect.) are only given for compounds with a preserved crystal structure.

Thermal Behavior

The thermal behavior of all synthesized compounds was determined by differential thermal analysis experiments. The compound with the highest decomposition temperature is the potassium salt **4**, which decomposes at a temperature of 281 °C. H_2DNPT (**3**) shows a clear decomposition at 207 °C (Figure 10). The other decomposition points are in a range of 168 °C for the 1,5-DATH derivative **5** and 240 °C for the tetraaminobitriazole salt (**8**). For the water containing compounds, the decomposition points for the hydrazinium (**10**·H_2O, 184 °C) and the hydroxylammonium (**11**·2 H_2O, 197 °C) com-

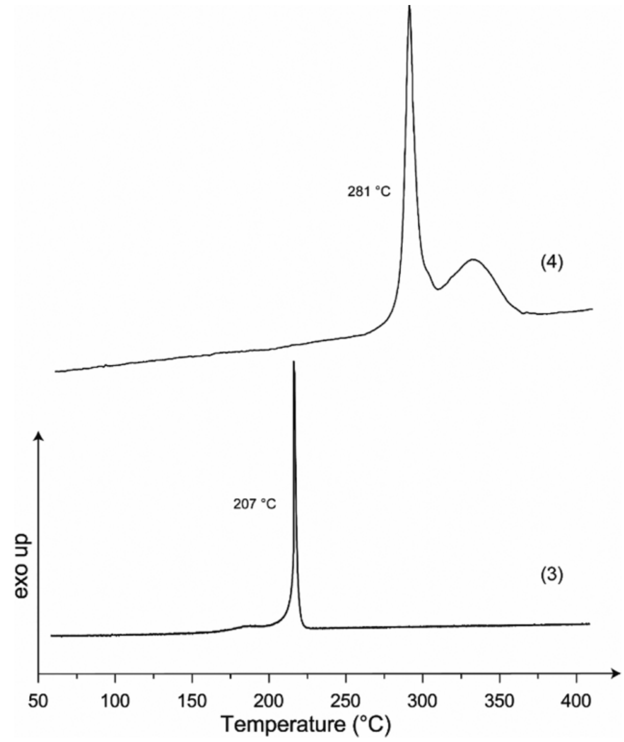

Figure 10. DTA plot of compounds **3** (bottom) and **4** (top) measured with a heating rate of 5 K·min^{-1}. Critical temperatures are given as onset temperature.

Table 3. Physic-chemical properties of compounds **3**–**5**, **7**, **8**, **11**, **12** and RDX.

	3	**4**	**5**	**7**	**8**	**11**·2 H_2O	**12**·2 H_2O	RDX
Formula	$C_4H_2N_8O_4$	$KC_4HN_8O_4$	$C_5H_6N_{14}O_4$	$C_5H_8N_{12}O_4$	$C_8H_{10}N_{18}O_4$	$C_4H_9N_9O_7$	$C_4H_9N_{10}O_6$	$C_3H_6N_6O_6$
M /g·mol^{-1}	226.11	264.21	326.20	300.20	422.29	295.17	279.17	222.12
IS /J [a)]	2.0	1.0	2.0	20	40	10	5	7.5
FS /N [b)]	120	20	192	360	>360	360	360	120
ESD /J [c)]	0.06	0.12	0.25	0.61	0.54	0.25	0.12	0.2
N /% [d)]	49.56	42.41	60.12	55.99	59.70	42.71	45.16	37.84
Ω /% [e]	–35.38	–30.28	–44.14	–53.29	–64.41	–29.81	–37.25	–21.61
$T_{dec.}$ /°C [f)]	207	281	168	209	240	197	254	210
Density (298 K) / g·cm^{-3} [g)]	1.669	1.879	1.757	1.713	1.729	1.685	1.667	1.800
$\Delta_f H_m°$ /kJ·mol^{-1} [h)]	517.1	305.5	820.6	432.7	298.	425.1	348.4	70.3
$\Delta_f U°$ /kJ·kg^{-1}] [i)]	2369.1	1219.6	2618.2	1557.0	816.4	1564.0	1374.5	433.7
Detonation parameters calculated with EXPLO5 V6.05								
$-\Delta_E U°$ /kJ·kg^{-1}] [j)]	5258	4842	4875	4190	2613.1	6240	5682	5740
T_E /K [k)]	4093	3591	3506	2997	2174	4010	3694	3745
p_{CJ} /kbar [l)]	260	236	279	243	188	310	283	336
V_D /m·s^{-1} [m)]	8062	7568	8441	8062	7364	8648	8431	8801
Gas vol. /L·kg^{-1} [n)]	752	537	786	808	773	833	845	711

a) Impact sensitivity (BAM drophammer, 1 of 6). b) Friction sensitivity (BAM friction tester, 1 of 6). c) Electrostatic discharge device (OZM). d) Nitrogen content. e) Oxygen balance. f) Decomposition temperature from DSC (β = 5 °C). g) Estimated from X-ray diffraction. h) Calculated (CBS-4M) heat of formation. i) Calculated energy of formation. j) Heat of explosion. k) Explosion temperature. l) Detonation pressure. m) Detonation velocity. n) Assuming only gaseous products.

pound are slightly below 200 °C; the ammonium salt (**12**·2 H_2O) reaches a value of 254 °C. The potassium derivative showed detonation-like decomposition in a hot plate test, in which 50 mg of **4** was heated on a copper plate with a bunsen burner. An initiation test, in which 50 mg of compound **4** was compressed onto 200 mg of PETN in a copper sleeve and an ignitor, which produced a jet of flame, did not initiate PETN but caused a deflagration.

Sensitivities

Additionally, the sensitivity values for external stimuli toward impact, friction and electrostatic discharge were determined following the BAM standards.[45–46] The potassium salt (**4**, IS = 1 J, FS = 20 N, ESD = 12 mJ) is the most sensitive compound containing the $HDNPT^-$ anion. The neutral compound **3** shows low values for the sensitivity towards impact of 2 J and electrostatic discharge of 60 mJ. The value for friction sensitivity is moderate with 120 N. Except the 1,5-DAT salt **5** (FS = 192 N), all nitrogen-rich salts are insensitive towards friction (FS = 360 N). Also in terms of impact sensitivity compound **5** (IS = 2 J) has the lowest value for nitrogen-rich derivatives. The other values vary from 5 J for the hydrazinium **10**·H_2O and ammonium **12**·2 H_2O compound to 40 J for insensitive salts **6**, **8** and **9**. Excluding the ammonium **12**·2 H_2O compound (ESD = 0.12 J), all other values for ESD sensitivity are $>$ 0.25 J.

Detonation Parameters

The detonation velocity V_D and pressure p_{CJ} were calculated using the EXPLO5 code. The densities used in the calculations were determined based on the respective crystal structures. However these values cannot compete with RDX (V_D = 8801 m·s^{-1}; p_{CJ} = 336 kbar). All compounds listed in Table 3 show a high positive heat of formation from 816.4 kJ·kg^{-1} for **8** to 2618.2 kJ·kg^{-1} for **5**, which clearly exceeds that of RDX (433.7 kJ·kg^{-1}). The water containing hydroxylammonium derivative **11** with V_D = 8648 m·s^{-1} and p_{CJ} = 310 kbar is the only compound that shows values close to those of RDX. The other compounds show calculated values in the range of 7364 m·s^{-1} (**8**) to 8441 m·s^{-1} (**5**) for the detonation velocity and 188 kbar (**8**) to 283 kbar (**12**·2 H_2O) for the detonation pressure. The neutral compound H_2DNPT (**3**) shows moderate values (V_D = 8062 m·s^{-1}; p_{CJ} = 260 kbar).

Conclusions

In this study, we report an innovative synthesis leading to a previously unknown C–C connection of a dinitropyrazole moiety with a tetrazole ring. The starting material for the synthesis was 4-amino-3,5-dinitropyrazole (ADNP, **1**), which can be produced from pyrazole in 3 steps via an established synthesis pathway. Subsequently, a diazotization of **1** to the intermediate diazonium compound takes place, which is immediately converted to 4-cyano-3,5-dinitropyrazole (**2**) by cyanide substitution. A final [2+3] cycloaddition reaction with sodium azide and zinc chloride as catalyst yields H_2DNPT (**3**). By reacting H_2DNPT (**3**) with nitrogen-rich organic bases and potassium carbonate, nine ionic derivatives were synthesized. All compounds were fully characterized via vibrational (IR) and NMR spectroscopy as well as sensitivity towards impact, friction and electrostatic discharge. The thermal behavior was investigated using differential thermal analysis (DTA), with the potassium derivative **4** with a T_{dec} = 281 °C being particularly striking. For certain compounds the detonation parameters were calculated with the EXPLO5 code using the corresponding crystal structure data. For the anhydrous compounds, the values range from 7364 m·s^{-1} for TABTrH compound **8** to 8441 m·s^{-1} for 1,5-DATH compound **5**. The neutral compound H_2DNPT (**3**) shows passable values for the detonation velocity and pressure (V_D = 8062 m·s^{-1}, p_{CJ} = 260 kbar). Unfortunately, the apparently most promising cations yield material with included water molecules. Dehydration of these compounds was not possible because water was immediately trapped again when the compounds were dried and then exposed to air again. For the hydroxylammonium salt **11** with two crystal water moieties, the value for V_D is still 8648 m·s^{-1}.

Experimental Section

General Procedures: ^{1}H, ^{13}C, ^{14}N and ^{15}N NMR spectra were recorded on JEOL 270 and BRUKER AMX 400 instruments. The samples were measured at room temperature in standard NMR tubes (Ø 5 mm). Chemical shifts are reported as d values in ppm relative to the residual solvent peaks of [D$_6$]DMSO (δ_H: 2.50, δ_C: 39.5). Solvent residual signals and chemical shifts for NMR solvents were referenced against tetramethylsilane (TMS, δ = 0 ppm) and nitromethane. Unless stated otherwise, coupling constants were reported in Hertz (Hz) and for the characterization of the observed signal multiplicities the following abbreviations were used: s (singlet), m (multiplet) and br (broad). Mass spectra were recorded on a JEOL MStation JMS700 using the EI or ESI technique. Infrared spectra (IR) were recorded from 4000 cm^{-1} to 400 cm^{-1} on a PERKIN ELMER Spectrum BX- 59343 instrument with a SMITHS DETECTION DuraSamplIR II Diamond ATR sensor. The absorption bands are reported in wave-numbers (cm^{-1}). Decomposition temperatures were measured via differential thermal analysis (DTA) with an OZM Research DTA 552-Ex instrument at a heating rate of 5 K·min^{-1} and in a range of room temperature to 400 °C. All sensitivities toward impact (IS) and friction (FS) were determined according to BAM (German: Bundesanstalt für Materialforschung und Prüfung) standards using a BAM drop hammer and a BAM friction apparatus by applying the 1 of 6 method. All energetic compounds were tested for sensitivity towards electrical discharge using an Electric Spark Tester ESD 2010 EN from OZM.

CAUTION! All investigated compounds are potentially explosive materials, although no hazards were observed during preparation and handling these compounds. Nevertheless, safety precautions (such as wearing leather coat, face shield, Kevlar sleeves, Kevlar gloves, earthed equipment and ear plugs) should be drawn.

Synthesis of Sodium 4-cyano-3,5-dinitropyrazolate dihydrate NaCDNP·2 H_2O (2): 4-Amino-3,5-dinitropyrazole (5.00 g, 28.9 mmol, 1.0 equiv.) was solved in sulfuric acid (200 mL, 1 M) and added to a solution of sodium nitrite (2.5 g, 36.2 mmol, 1.3 equiv.) in water

Journal of Inorganic and General Chemistry
ZAAC
Zeitschrift für anorganische und allgemeine Chemie

(50 mL) at 5 °C. The mixture was stirred for 20 min at this temperature and further stirred at ambient temperature for 30 min. The mixture was neutralized with sodium hydrogen carbonate to pH = 7. Then, copper(I)-cyanide (3.20 g, 35.7 mmol, 1.2 equiv.) was added in one portion and a solution of sodium cyanide (2.50 g, 51.0 mmol, 1.8 equiv.) in water (50 mL) was added dropwise to the mixture. The solution was then stirred for 30 min at room temperature and for 2 h at 70 °C. Afterwards, the mixture was cooled to room temperature and the precipitated solid was filtered and discarded. The solvent was evaporated under reduced pressure and the brown residue was extracted with ethyl acetate (400 mL). The organic layer was dried with anhydrous sodium sulfate and the solvent was evaporated under reduced pressure to yield sodium 4-cyano-3,5-dinitropyrazolate dihydrate (**2**) (5.80 g, 24.1 mmol, 83 %) as brown solid. DTA (5 K·min^{-1}): 77 °C (endo), 210 °C (dec.). **IR** (ATR): $\tilde{\nu}$ = 3574(m), 3566(m), 3390(w), 3378(m), 3325(w), 3307(w), 3280(w), 3206(w), 2249(w), 1636(m), 1534(s), 1512(s), 1504(s), 1455(s), 1430(m), 1414(s), 1361(s), 1324(vs), 1239(m), 1185(m), 1145(m), 1130(m), 1044(m), 1044(m), 1024(m), 1016(m), 1003(m), 847(s), 805(m), 767(m), 744(m), 719(m), 693(s), 641(s), 544(s), 500(s), 493(s) cm^{-1}. $C_4H_4N_5O_6Na$ (241.09 g·mol^{-1}): calcd.: C 19.43, N 28.21, H 1.69 %; found: C 19.93, N 29.05, H 1.67 %. **^{1}H NMR** ([D$_6$]DMSO, 400 MHz, ppm): δ = 3.44 (s, 4 H). **^{13}C NMR** ([D$_6$]DMSO, 101 MHz, ppm): δ = 156.9, 111.7, 82.5. **^{14}N NMR** ([D$_6$]DMSO, 29 MHz, ppm): δ = –22; *m/z* (ESI$^-$): 182 (anion).

Synthesis of 5-(3,5-dinitro-1*H*-pyrazol-4-yl)-1*H*-tetrazole H_2DNPT (3): Sodium 4-cyano-3,5-dinitropyrazolate dihydrate (5.80 g, 24.1 mmol, 1.0 equiv.) was solved in water (400 mL) and sodium azide (4.70 g, 72.3 mmol, 3.0 equiv.) and zinc chloride (9.85 g, 72.3 mmol, 3.0 equiv.) were added and the solution was stirred for 72 h at 85 °C. Afterwards, the residue was filtered off, solved in hydrochloric acid (200 mL, 2 M) and extracted with ethyl acetate (4 × 100 mL). The organic phase was dried with anhydrous sodium sulfate and the solvent was evaporated under reduced pressure. The resulting viscous mass was solved in toluene/acetone (1:1, 20 mL) and the solvent was evaporated under reduced pressure. The procedure was repeated twice to yield 5-(3,5-dinitro-1*H*-pyrazol-4-yl)-1*H*-tetrazole (**3**) (3.00 g, 13.3 mmol, 55 %) as a slightly brown powder. DTA (5 K·min^{-1}): 207 °C (dec.); Sensitivities: BAM drop hammer: 2 J (500–1000 µm), friction tester: 120 N (500–1000 µm), ESD: 60 mJ (500–1000 µm). **IR** (ATR): $\tilde{\nu}$ = 3217(w), 2921(m), 2703(m), 2622(m), 1886(w), 1645(w), 1533(s), 1505(s), 1437(m), 1416(s), 1399(s), 1388(s), 1357(s), 1323(vs), 1295(m), 1279(m), 1253(m), 1218(m), 1182(w), 1156(m), 1149(m), 1114(w), 1088(m), 1088(m), 1070(m), 1028(m), 1016(m), 988(s), 854(s), 840(vs), 772(m), 755(m), 715(m), 675(m), 659(m), 637(m), 624(m), 560(m), 514(m), 477(w), 430(m), 416(m), 408(m) cm^{-1}. $C_4H_2N_8O_4$ (226.11 g·mol^{-1}): calcd.: C 21.25, N 49.56, H 0.89 %; found: C 21.13, N 49.21, H 0.87 %. **^{1}H NMR** ([D$_6$]DMSO, 400 MHz, ppm): δ = 14.24 (br. s, 2 H). **^{13}C NMR** ([D$_6$]DMSO, 101 MHz, ppm): δ = 153.6, 147.3, 97.5. **^{14}N NMR** ([D$_6$]DMSO, 29 MHz, ppm): δ = –24. **^{15}N NMR** ([D$_6$]DMSO, 41 MHz, ppm): δ = –9.5, –25.4, –93.8, –98.0; *m/z* (ESI$^-$): 225 (anion).

Crystallographic data (excluding structure factors) for the structures in this paper have been deposited with the Cambridge Crystallographic Data Centre, CCDC, 12 Union Road, Cambridge CB21EZ, UK. Copies of the data can be obtained free of charge on quoting the depository numbers CCDC-1985990 (for **2**), CCDC-1985991 (for **3**), CCDC-1985993 (for **4**), CCDC-1985992 (for **5**) CCDC-1985996 (for **7**) CCDC-1985997 (for **8**) CCDC-1985994 (for **11**·2 H_2O), and CCDC-1985995 (for **12**·2 H_2O) (Fax: +44-1223-336-033; E-Mail: deposit@ccdc.cam.ac.uk, http://www.ccdc.cam.ac.uk).

Supporting Information (see footnote on the first page of this article): 1) X-ray Diffraction Tables, 2) Computations, 3) Experimental Details.

Acknowledgements

For financial support of this work by the Ludwig-Maximilian University (LMU), the Office of Naval Research (ONR) under grant no. ONR N00014–19–1-2078 and the Strategic Environmental Research and Development Program (SERDP) under contract no. W912HQ19C0033 are gratefully acknowledged. The authors thank *Stefan Huber* for his help with the sensitivity measurement and *Florian Kris* for synthetic assistance. Open access funding enabled and organized by Projekt DEAL.

Keywords: Energetic material; Pyrazoles; Tetrazoles; Polynitro azoles; Structure elucidation

References

[1] B. Palaszewski, L. S. Ianovski, P. Carrick, *J. Propul. Power* **1998**, *14*, 641–648.
[2] S. B. Kim, K. J. Kim, M. H. Cho, J. H. Kim, K. T. Kim, S. H. Kim, *ACS Appl. Mater. Interfaces* **2016**, *8*, 9405–9412.
[3] H. Gao, J. M. Shreeve, *Chem. Rev.* **2011**, *111*, 7377–7436.
[4] Z. L. Chioato, T. M. Klapötke, F. Mieskes, J. Stierstorfer, M. Weyrauther, *Eur. J. Inorg. Chem.* **2016**, 956–962.
[5] T. M. Klapötke, *Chemistry of High-Energy Materials*, De Gruyter, Boston, Berlin, **2017**.
[6] M. R. Manaa, E. J. Reed, L. E. Fried, N. Goldman, *J. Am. Chem. Soc.* **2009**, *131*, 5483–5487.
[7] E.-C. Koch, *Propellants Explos. Pyrotech.* **2015**, *40*, 374–387.
[8] G. Wang, T. Lu, G. Fan, H. Yin, F.-X. Chen, *New J. Chem.* **2019**, *43*, 1663–1666.
[9] T. Brinck, *Green Energetic Materials*, Wiley, Hoboken, **2014**.
[10] D. Fischer, J. L. Gottfried, T. M. Klapötke, K. Karaghiosoff, J. Stierstorfer, T. G. Witkowski, *Angew. Chem. Int. Ed.* **2016**, *55*, 16132–16135.
[11] C.-J. Lei, H.-W. Yang, H.-L. Xiong, G.-B. Cheng, *Propellants Explos. Pyrotech.* **2019**, *44*, 1–7.
[12] D. Fischer, T. M. Klapötke, M. Reymann, J. Stierstorfer, *Chem. Eur. J.* **2014**, *20*, 6401–6411.
[13] W. Fu, B. Zhao, M. Zhang, C. Li, H. Gao, J. Zhang, Z. Zhou, *J. Mater. Chem. A* **2017**, *5*, 5044–5054.
[14] N. Fischer, D. Fischer, T. M. Klapötke, D. G. Piercey, J. Stierstorfer, *J. Mater. Chem.* **2012**, *22*, 20418–20422.
[15] J. Zhang, J. M. Shreeve, *J. Am. Chem. Soc.* **2014**, *136*, 4437–4445.
[16] J. Zhang, P. Yin, G. Pan, Z. Wang, J. Zhang, L. A. Mitchell, D. A. Parrish, J. n. M. Shreeve, *New J. Chem.* **2019**, *43*, 12684–12689.
[17] M. F. Bölter, T. M. Klapötke, T. Kustermann, T. Lenz, J. Stierstorfer, *Eur. J. Inorg. Chem.* **2018**, *2018*, 4125–4132.
[18] A. A. Dippold, T. M. Klapötke, *Chem. Asian J.* **2013**, *8*, 1463–1471.
[19] A. A. Dippold, D. Izsák, T. M. Klapötke, *Chem. Eur. J.* **2013**, *19*, 12042–12051.
[20] P. F. Pagoria, M.-X. Zhang, N. B. Zuckerman, A. J. DeHope, D. A. Parrish, *Chem. Heterocycl. Compd.* **2017**, *53*, 760–778.
[21] E. C. Johnson, J. J. Sabatini, D. E. Chavez, R. C. Sausa, E. F. C. Byrd, L. A. Wingard, P. E. Guzmàn, *Org. Process Res. Dev.* **2018**, *22*, 736–740.
[22] D. Fischer, J. L. Gottfried, T. M. Klapötke, K. Karaghiosoff, J. Stierstorfer, T. G. Witkowski, *Angew. Chem. Int. Ed.* **2016**, *55*, 16132–16135.
[23] P. Yin, L. A. Mitchell, D. A. Parrish, J. M. Shreeve, *Angew. Chem.* **2016**, *128*, 14621–14623.

[24] R. Yang, Z. Dong, Z. Ye, *ChemistrySelect* **2019**, *4*, 14208–14213.
[25] J. C. Galvez-Ruiz, G. Holl, K. Karaghiosoff, T. M. Klapötke, K. Loehnwitz, P. Mayer, H. Noeth, K. Polborn, C. J. Rohbogner, M. Suter, J. J. Weigand, *Inorg. Chem.* **2005**, *44*, 5192–5192.
[26] K. V. Domasevitch, I. Gospodinov, H. Krautscheid, T. M. Klapötke, J. Stierstorfer, *New J. Chem.* **2019**, *43*, 1305–1312.
[27] T. K. Shkineva, A. V. Kormanov, V. N. Boldinova, I. A. Vatsadze, I. L. Dalinger, *Chem. Heterocycl. Compd.* **2018**, *54*, 703–709.
[28] D. Kumar, G. H. Imler, D. A. Parrish, J. M. Shreeve, *New J. Chem.* **2017**, *41*, 4040–4047.
[29] S. Ek, N. V. Latypov, *J. Heterocycl. Chem.* **2014**, *51*, 1621–1627.
[30] I. L. Dalinger, I. A. Vatsadze, T. K. Shkineva, G. P. Popova, S. A. Shevelev, *Mendeleev Commun.* **2012**, *22*, 43–44.
[31] I. L. Dalinger, I. A. Vatsadze, T. K. Shkineva, G. P. Popova, S. A. Shevelev, *Synthesis* **2012**, *44*, 2058–2064.
[32] Z. P. Demko, K. B. Sharpless, *J. Org. Chem.* **2001**, *66*, 7945–7950.
[33] H. Huang, Z. Zhou, L. Liang, J. Song, K. Wang, D. Cao, C. Bian, W. Sun, M. Xue, *Z. Anorg. Allg. Chem.* **2012**, *638*, 392–400.
[34] L. Liang, H. Huang, K. Wang, C. Bian, J. Song, L. Ling, F. Zhao, Z. Zhou, *J. Mater. Chem.* **2012**, *22*, 21954–21964.
[35] V. D. Ghule, S. Radhakrishnan, P. M. Jadhav, *Struct. Chem.* **2011**, *22*, 775–782.
[36] A. F. Hollemann, E. Wiberg, N. Wiberg, *Lehrbuch der anorganischen Chemie*, de Gruyter: New York, **2007**.
[37] M. Dachs, A. A. Dippold, J. Gaar, M. Holler, T. M. Klapötke, *Z. Anorg. Allg. Chem.* **2013**, *639*, 2171–2180.
[38] F. H. Allen, O. Kennard, D. G. Watson, L. Brammer, A. G. Orpen, R. Taylor, *J. Chem. Soc.* **1987**, 1–19.
[39] M. Tariq, S. Hameed, I. H. Bechtold, A. J. Bortoluzzi, A. A. Merlo, *J. Mater. Chem. C* **2013**, *1*, 5583–5593.
[40] M. F. Bölter, A. Harter, T. M. Klapötke, J. Stierstorfer, *ChemPlusChem.* **2018**, *83*, 804–811.
[41] N. Fischer, T. M. Klapötke, M. Reymann, J. Stierstorfer, *Eur. J. Inorg. Chem.* **2013**, 2167–2180.
[42] M. J. Frisch, G. W. Trucks, H. B. Schlegel, G. E. Scuseria, M. A. Robb, J. R. Cheeseman, G. Scalmani, V. Barone, B. Mennucci, G. A. Petersson, H. Nakatsuji, M. Caricato, X. Li, H. P. Hratchian, A. F. Izmaylov, J. Bloino, G. Zheng, J. L. Sonnenberg, M. Hada, M. Ehara, K. Toyota, R. Fukuda, J. Hasegawa, M. Ishida, T. Nakajima, Y. Honda, O. Kitao, H. Nakai, T. Vreven, J. A. Montgomery Jr., J. E. Peralta, F. Ogliaro, M. Bearpark, J. J. Heyd, E. Brothers, K. N. Kudin, V. N. Staroverov, T. Keith, R. Kobayashi, J. Normand, K. Raghavachari, A. Rendell, J. C. Burant, S. S. Iyengar, J. Tomasi, M. Cossi, N. Rega, J. M. Millam, M. Klene, J. E. Knox, J. B. Cross, V. Bakken, C. Adamo, J. Jaramillo, R. Gomperts, R. E. Stratmann, O. Yazyev, A. J. Austin, R. Cammi, C. Pomelli, J. W. Ochterski, R. L. Martin, K. Morokuma, V. G. Zakrzewski, G. A. Voth, P. Salvador, J. J. Dannenberg, S. Dapprich, A. D. Daniels, O. Farkas, J. B. Foresman, J. V. Ortiz, J. Cioslowski, and D. J. Fox, *Gaussian 09 Revision C.01*, Gaussian, Inc., Wallingford, CT, USA, **2010**.
[43] J. Stierstorfer, *Dissertation*, Ludwig-Maximilians-Universität München, **2009**.
[44] M. Hesse, H. Meier, B. Zeeh, in: *Spektroskopische Methoden in der organischen Chemie*, Vol. 6, Thieme, Stuttgart, New York, **2002**.
[45] Reichel & Partner GmbH, http://www.reichelt-partner.de.
[46] Test Methods According to the UN Recommendations on the Transport of Dangerous Goods, Manual of Test and Criteria, Fourth Revised Edition, United Nations Publication, New York and Geneva, 2003, ISBN 92–1-139087 7, Sales No. E.03.VIII. 2; 13.4.2 Test 3a (ii) BAM Fallhammer.

Received: March 10, 2020
Published Online: June 18, 2020

